ELSEVIER

Carbohydrate Research 303 (1997) 79–92

CARBOHYDRATE RESEARCH

Structural characterisation of galactoglucomannan secreted by suspension-cultured cells of *Nicotiana plumbaginifolia*

Ian M. Sims [a,1], David J. Craik [b], Antony Bacic [a,*]

[a] *Cooperative Research Centre for Industrial Plant Biopolymers and Plant Cell Biology Research Centre, School of Botany, University of Melbourne, Parkville, Victoria 3052, Australia*

[b] *Centre for Drug Design and Development, University of Queensland, St. Lucia, Queensland 4072, Australia*

Received 4 February 1997; accepted 28 April 1997

Abstract

Galactoglucomannan (GGM) from cultures of *Nicotiana plumbaginifolia* has Man:Glc:Gal:Ara:Xyl in 1.0:1.1:1.0:0.1:0.04 ratio. Linkage analysis contained 4- and 4,6-Man*p*, 4-Glc*p*, terminal Gal*p* and 2-Gal*p*, small amounts and terminal Ara*p* and terminal Xyl*p*, and ~ 0.03 mol acetyl per mol of glucosyl residue. Treatment with α- and β-D-galactosidases showed that the majority of the side-chains were either single Gal*p*-α-(1 → residues or the disaccharide Gal*p*-β-(1 → 2)-Gal*p*-α-(1 → linked to O-6 of the 4-Man*p* residues of the glucomannan backbone. Analysis of the oligosaccharides generated by endo-(1 → 4)-β-mannanase digestion confirmed that the GGM comprises a backbone of predominantly alternating → 4)-D-Man*p*-β-(1 → and → 4)-D-Glc*p*-β-(1 → branched at O-6 of 65% of the 4-Man*p* residues. The major oligosaccharide identified was D-Glc*p*-β-(1 → 4)-[D-Gal*p*-β-(1 → 2)-D-Gal*p*-α-(1 → 6)]-D-Man*p*-β-(1 → 4)-D-Glc*p*-β-(1 → 4)-[D-Gal*p*-α-(1 → 6)]-D-Man*p*-β-(1 → (27%), and most of the other oligosaccharides produced in significant quantities were based on this structure. © 1997 Elsevier Science Ltd.

Keywords: *Nicotiana plumbaginifolia*; Galactoglucomannan; Endo-(1 → 4)-β-mannanase; Linkage analysis; Electrospray ionisation–mass spectrometry; Nuclear magnetic resonance; Plant cell culture

1. Introduction

(Galacto)glucomannans (GGMs) are a family of polysaccharides with backbones of both (1 → 4)-β-D-Glc*p* and (1 → 4)-β-D-Man*p* residues, that occur primarily in the lignified secondary walls of gymnosperms and, to a lesser extent, angiosperms [1] and in the walls of the endosperm of some seeds [2]. The ratio of Man:Glc:Gal for GGMs is variable, but is

Abbreviations: GGM, galactoglucomannan; XG, xyloglucan; ESI–MS, electrospray ionisation–mass spectrometry; GC–MS, gas chromatography–mass spectrometry; NMR, nuclear magnetic resonance; amu, atomic mass units; ppm, parts per million; RT, retention time; Da, daltons

* Corresponding author.

[1] Current address: Industrial Research Ltd., Gracefield Research Centre, Gracefield Road, PO Box 31-310, Lower Hutt, New Zealand.

PII S0008-6215(97)00144-4

commonly about 3:1:1 from gymnosperms [1,2], 5:4:1 from the endosperm of asparagus seeds, 11:1:2 from the endosperm of the Judas tree [2], and 10:4:1 from poplar wood [3]. Analysis of the products of partial hydrolysis of GGM suggests that the distribution of →4)-D-Man*p*-β-(1→ and →4)-D-Glc*p*-β-(1→ residues in the backbone is non-regular; →4)-D-Man*p*-β-(1→ residues can be adjacent to each other, but →4)-D-Glc*p*-β-(1→ residues are not. Only the →4)-D-Man*p*-β-(1→ residues are substituted with D-Gal*p* substituents [2]. *O*-Acetyl substitution of the glucomannan backbone also appears to be common on the GGMs from the secondary cell walls of coniferous woods [4].

GGMs have been reported to occur in the primary cell walls of *Nicotiana tabacum* (tobacco) and *Rubus fruticosus* (blackberry), and are secreted into the extracellular medium of suspension-cultured cells of these two species [5–7]. These GGMs differ from those of secondary cell walls by containing almost equal proportions of Man:Glc:Gal, and they appear to consist of a backbone of alternating →4)-D-Man*p*-β-(1→ and →4)-D-Glc*p*-β-(1→ residues branched at O-6 of the Man*p* residues to side-chains of Gal*p* residues [5–7]. For GGM from ECPs of suspension-cultured *N. tabacum* cells side-chains were attached to O-6 of ~66% of the →4)-D-Man*p*-β-(1→ residues, and were shown to be composed of either Gal*p*-α-(1→ residues or Gal*p*-β-(1→2)-Gal*p*-α-(1→ disaccharides. Terminal Ara*f* and terminal Xyl*p* residues present in glycosyl linkage analyses of GGM were not detected in oligosaccharide fractions. We have recently isolated a GGM from the extracellular medium of suspension-cultured cells of *N. plumbaginifolia* [8], which has a similar linkage composition to GGM secreted into the medium of suspension-cultured *N. tabacum* cells [5]. However, the GGM from *N. plumbaginifolia* contains about half as much 2-Gal*p* as GGM from *N. tabacum*, and contains a small proportion (2 mol%) of terminal Ara*p* residues, not detected in GGM from *N. tabacum*.

In this paper, we report the detailed structure of GGM secreted by *N. plumbaginifolia* suspension cultures. The composition of the side-chains was determined by treatment with α- and β-galactosidases. The major oligosaccharides produced by digestion of GGM with endo-(1→4)-β-mannanase were separated by a combination of gel-filtration chromatography and anion-exchange HPLC, and analysed by methylation analysis, electrospray ionisation–mass spectrometry (ESI–MS), and proton-nuclear magnetic resonance (^{1}H NMR).

2. Experimental

Purification of GGM.—GGM was isolated from ECPs of *N. plumbaginifolia* using a combination of anion-exchange chromatography and treatment of neutral polysaccharides with satd $(NH_4)_2SO_4$ [8] and is designated the native GGM preparation. This preparation contained ~24% xyloglucan (XG); the XG can be removed by precipitation of GGM with satd $Ba(OH)_2$, but this results in *O*-deacetylation of the GGM and was thus not used in this study. Since the detailed structure of this XG was known [9] this contamination did not pose any difficulties in interpretation of the data for GGM.

Enzymic digestion of GGM.—Native GGM (100 μg) was dissolved in 20 mM NH_4OAc (1 mL, pH 4.5) and digested with either α-D-galactosidase from *Cyanopsis tetragonobolus* (guar; 0.2 mg protein, 15 Units, Megazyme, Ireland), or β-D-galactosidase from *Aspergillus niger* (0.2 mg protein, 8 Units, Megazyme), or with a combination of both enzymes at 40 °C for 24 h. The reactions were stopped by heating at 100 °C for 5 min, and the products precipitated by the addition of 4 vol of EtOH and freeze-dried.

Native GGM (10 mg) was dissolved in 20 mM NH_4OAc (10 mL, pH 4.5) and incubated with endo-(1→4)-β-mannanase from *A. niger* (1.4 mg protein, 10 Units, Megazyme) at 40 °C. Fractions (1 mL) were removed at intervals and the reaction stopped by heating at 100 °C for 5 min. Undigested material was removed by the addition of 4 vol of EtOH, and the 80% EtOH-soluble oligosaccharides were concd under reduced pressure at 40 °C, and freeze-dried. Digestion of the GGM was monitored by anion-exchange HPLC (see below).

Gel - filtration chromatography.—GGM oligosaccharides soluble in 80% EtOH (10 mg) were dissolved in deionised water (1 mL) and oligosaccharides separated on a column (190 × 2.2 cm i.d.) of Fractogel TSK HW-40(S) (E. Merck, Darmstadt, Germany) [9]. Fractions (4 mL) were tested for carbohydrate (see below) and those corresponding to individual oligosaccharide size-classes were pooled, concd under reduced pressure at 40 °C, and freeze-dried. The column was calibrated with a series of (1→4)-β-D-oligoglucosides prepared by acid hydrolysis of cellulose (Sigma) in 2.5 M TFA for 10 min at 100 °C [10].

Anion - exchange chromatography.—Mixtures of total unfractionated native GGM oligosaccharides (100 μg), or individual peaks from the gel-filtration

column (100 μg) were dissolved in deionised water (1 μg μL^{-1}) and separated by anion-exchange HPLC at a flow rate of 1 mL min^{-1} on a Dionex BioLC using a CarboPac PA-1 column (4 × 250 mm; Dionex Corp., Sunnyvale, CA, USA) equilibrated in 150 mM NaOH. Oligosaccharides were eluted with a linear gradient of NaOAc (0–250 mM) in 150 mM NaOH over 100 min, starting 5 min after sample injection, and monitored using pulsed amperometric detection (Dionex). Peak fractions were collected and neutralised with HOAc immediately after collection. Sodium ions were removed on a Dowex 50W-X8, H^+ column (Bio-Rad Laboratories) at 4 °C, and the purified oligosaccharides freeze-dried.

Analytical methods.—Total carbohydrate was determined by the phenol–H_2SO_4 method [11] using glucose (0–80 μg) as the standard.

Electrospray – mass spectrometry (ESI – MS).—ESI–MS spectra of methylated (see below) oligosaccharides were acquired using a Finnigan (Bremen, Germany) electrospray source attached to a Finnigan MAT 95 double-focussing negative sector mass spectrometer [12], and scanning from 100–2500 amu at 15 decade s^{-1}.

Linkage analysis.—Methylation under basic conditions was performed using the NaOH method [13]. Samples (10–100 μg) were dissolved in Me_2SO (50 μL) and methylated, extracted and dried [12]. For oligosaccharide samples the procedure was modified slightly with first aliquot of CH_3I being added immediately after the addition of the NaOH slurry.

To determine the positions of both the glycosidic linkages and the *O*-acetyl groups, samples were methylated first under neutral conditions using the method of [14], and resuspended in Me_2SO and remethylated with CD_3I under basic conditions (see above). In this way free hydroxyl groups were substituted with CH_3 groups during the neutral methylation procedure, and acetylated hydroxyl groups were then deacetylated and substituted with CD_3 groups during the base-catalysed methylation procedure [9].

Permethylated carbohydrates were either analysed directly by ESI–MS (see above) or hydrolysed with 2.5 M TFA (2 h, 100 °C), reduced with 1 M $NaBD_4$ overnight at room temperature and acetylated with Ac_2O (2 h, 100 °C) for linkage analysis. The resulting partially methylated alditol acetates were separated by GC on a fused-silica capillary column (25 m × 0.22 mm i.d.) with a high-polarity bonded phase BPX70 (SGE, Australia) and analysed by MS using a Finnigan MAT 1020B (San Jose, CA, USA) GC–MS [15].

NMR spectroscopy.—GGM oligosaccharides were dissolved in 540 μL of D_2O (99.96 atom%), in 5-mm NMR tubes (Wilmad Glass Co., 535-PP). Spectra were recorded on a Bruker DMX750 spectrometer operating at a ^1H frequency of 750 MHz. All spectra were recorded at 27 °C. The probe temperature was controlled using air flow from a BCU refrigerated temperature regulator. Chemical shifts were measured relative to internal acetone at δ 2.225 ppm [16].

1D NMR spectra were recorded using 16K data points over a spectral width of 6000 Hz (acquisition time 1.3 s). The spectra were acquired from the accumulation of 32–512 scans depending on the amount of each compound available. The total relaxation delay between 60° pulses was 3.3 s. Spectra were processed using an exponential multiplication window function which produced a line broadening of 0.3 Hz.

2D spectra were recorded in phase-sensitive mode using time-proportional phase incrementation [17]. The 2D experiments used included double quantum filtered scalar correlated spectroscopy (DFQ-COSY) [18] and total correlation spectroscopy (TOCSY) [19,20] recorded with a mixing time of 80 ms. The 2D spectra were acquired with 512 t_1 increments. The ^1H spectral widths were typically 2500 Hz in both dimensions, over 4K complex data points in F_2. During processing, data from the 2D spectra were zero-filled in F_1 to at least 1K data points. Either a 90° or 60° phase-shifted sine bell of sine bell squared window was applied to the data in both dimensions. Polynomial baseline correlation was applied in selected regions of each spectrum. All processing was performed using standard Bruker software (UXNMR) on a Silicon Graphics Indy workstation.

3. Results and discussion

Composition of GGM.—Linkage analysis of the native GGM preparation from *N. plumbaginifolia* ECPs, by methylation under basic conditions, revealed mostly 4-Man*p* and 4,6-Man*p*, 4-Glc*p* and 4,6-Glc*p*, terminal Gal*p* and 2-Gal*p*, together with smaller amounts of terminal Ara*f* and terminal Ara*p*, terminal Xyl*p* and 2-Xyl*p* (Table 1). From our knowledge of the structure of the XG purified from *N. plumbaginifolia* ECPs which is composed of 4,6-Glc*p* and 4-Glc*p* (equal to 1.5 times the amount of 4,6-Glc*p*), terminal Xyl*p* and 2-Xyl*p*, and terminal Ara*f* [8,9], we can deduce that the GGM preparation

Table 1
Linkage composition of native *Nicotiana plumbaginifolia* GGM and after treatment with α- and β-galactosidase

Sugar	Deduced glycosidic linkage [a]	Linkage composition (mol%) [b]			
		Native	α-Galase	β-Galase	α- + β-Galase
Ara*f*	Terminal	3	4	5	7
	Terminal *p*	2	3	3	4
	5-	1	2	2	1
Xyl*p*	Terminal	3	3	4	6
	2-	4	4	4	6
Man*p*	4-	8	14	8	23
	4,6-	15	10	15	3
Gal*p*	Terminal	16	10	18	1
	2-	7	8	1	tr [c]
Glc*p*	Terminal	1	2	2	3
	4-	34	35	34	39
	4,6-	6	5	4	6

[a] Terminal Ara*f* is deduced from 1,4-di-*O*-acetyl-2,3,5-tri-*O*-methylpentitol, etc.
[b] Average of duplicate determinations.
[c] tr, less than 1 mol%.

contained ~ 24 mol% XG that was not precipitated by satd $(NH_4)_2SO_4$. The GGM component of this preparation was thus deduced to be composed of 4-Man*p* and 4,6-Man*p*, 4-Glc*p* (25 mol%), terminal Gal*p* and 2-Gal*p*, and terminal Ara*p*; subsequently some of the terminal Xyl*p* (1 mol%) was also determined to be part of the GGM. The GGM comprised ~ 74% of the preparation and the ratio of Man:Glc:Gal:Ara:Xyl was calculated as 1.0:1.1:1.0:0.1:0.04.

Native GGM was also methylated under neutral conditions, and remethylated with CD_3I under basic conditions to determine the presence and position of alkali labile, presumably *O*-acetyl groups [9]. Thus the derivatives formed were a combination of partially methylated, partially deuteriomethylated, alditol acetates. In addition to the diagnostic ions for the terminal Gal*p* partially methylated alditol acetate derivative, a primary fragment at *m/z* 208, rather than *m/z* 205 (and the respective secondary fragment ions) indicated that a CD_3 group was present at O-6 of ~ 10% (from the ratio of *m/z* 205 to *m/z* 208) of the derivatives from this residue. Similarly, in the 4-Man*p* and 4-Glc*p* derivatives, primary fragment ions at *m/z* 236, rather than *m/z* 233 [9] (and the respective secondary fragment ions) indicated that CD_3 groups were present at *O*-6 of ~ 5% (from the ratios of *m/z* 233 to *m/z* 236) of the derivatives from both of these residues. From these results the degree of *O*-acetylation of terminal Gal*p* from the GGM was calculated to be 10 mol% and the degree of *O*-acetylation of 4-Man*p* from the GGM was calculated to be 5 mol%. We were unable to establish whether the *O*-acetylation on the terminal Gal*p* residues was on terminal Gal*p*-α-(1 → or terminal Gal*p*-β-(1 → or both since deacetylation had occurred in the purified oligosaccharides. Due to the presence of XG in this preparation it was not possible to unequivocally assign the CD_3 groups detected on the 4-Glc*p* residue to GGM, but based on data for *N. plumbaginifolia* XG [9], in which *O*-acetyl groups are present on ~ 44% of 4-Glc*p* residues, *O*-acetyl substitution of 4-Glc*p* in GGM would be negligible. Thus, the total degree of *O*-acetylation of the GGM calculated from the degree of *O*-acetylation of terminal Gal*p* (16 mol% × 0.10) and 4-Man*p* (8 mol% × 0.05) was ~ 0.03 mol acetyl per mol of glycosyl residue (where GGM represents ~ 74 mol% of the preparation), which is equivalent to ~ 0.8% w/w (where the molecular weight of a glycosyl residue in a polymer is taken as 162 Da).

Enzyme digestion of GGM.—Digestion for 24 h of native GGM with α-D-galactosidase removed ~ 38% of the terminal Gal*p* residues (16 to 10 mol%), and was accompanied by a decrease in the amount of 4,6-Man*p* (15 to 10 mol%) and a corresponding increase in the amount of 4-Man*p* (8 to 14 mol%) (Table 1). Further incubation of the GGM with α-D-galactosidase did not remove the remaining terminal Gal*p* residues. XG from *N. plumbaginifolia* ECPs

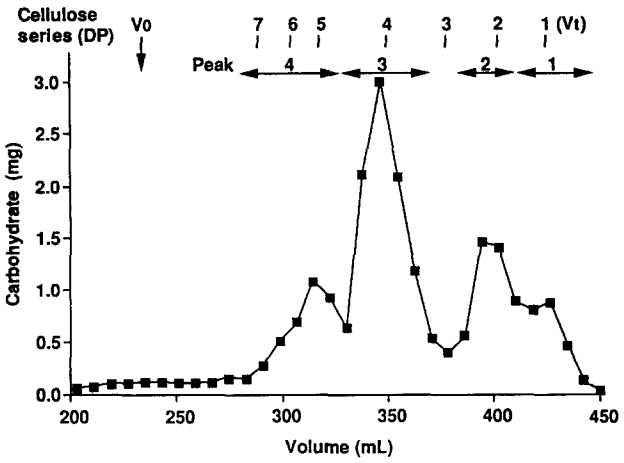

Fig. 1. Gel-filtration chromatography on a Fractogel TSK HW-40 column of native *Nicotiana plumbaginifolia* GGM digested with endo-(1 → 4)-β-mannanase. The total carbohydrate content of each fraction (4 mL) was determined by the phenol–H_2SO_4 assay. The column was calibrated with a series of (1 → 4)-β-D-oligoglucosides (dp 1–7). Fractions (1–3) were collected for further fractionation and analysis; fraction 4 contained partially digested GGM.

contains only minor amounts of terminal D-Gal*p*-β-(1 → (1 mol% total polysaccharide) [9], and thus the majority of terminal Gal*p* residues remaining after treatment with α-D-galactosidase must be side-chains on GGM that are not susceptible to this enzyme.

Digestion for 24 h of native GGM with β-D-galactosidase removed almost all of the 2-Gal*p* residues (7 to 1 mol%), but did not alter significantly the proportions of terminal Gal*p*, 4-Man*p* and 4,6-Man*p* (Table 1). Further incubation of the GGM with β-D-galactosidase did not remove any Gal*p* residues. This suggested that terminal D-Gal*p*-β-(1 → residues were attached to 2-Gal*p* residues which were not susceptible to β-D-galactosidase following removal of the terminal D-Gal*p*-β-(1 → residues.

When GGM was digested for 24 h with both α- and β-galactosidase almost all of the terminal Gal*p* and 2-Gal*p* was removed (23 to 1 mol%), and 4,6-Man*p* was reduced by ~ 80% (from 15 to 3 mol%), while the proportion of 4-Man*p* increased from 8 to 23 mol%. The increase in the amount of 4-Glc*p* (34 to 39 mol%) was attributed to the removal of Gal*p* residues (22 mol%) resulting in a general increase in the amounts of all the remaining residues, and did not indicate that any terminal Gal*p* residues were attached to 4,6-Glc*p*. The amount of terminal Ara*p* (4 mol%) remaining after digestion with both α- and β-galactosidase was almost equal to the amount of 4,6-Man*p* (3 mol%; Table 1).

From these results it was calculated that ~ 38% of the side-chains attached to O-6 of 4-Man*p* were D-Gal*p*-α-(1 → , and that ~ 42% were D-Gal*p*-β-(1 → 2)-D-Gal*p*-α-(1 → . The remaining 20% of side-chains attached to O-6 of 4-Man*p* were deduced to comprise Ara*p* and, subsequently, Xyl*p* residues (see later).

In order to establish the structures of the oligosaccharide repeats in GGM the native GGM was digested with endo-(1 → 4)-β-mannanase. Digestion was complete after 24 h, with 87% (w/w) soluble in 80% (v/v) ethanol. Further incubation with endo-(1 → 4)-β-mannanase did not increase the proportion of ethanol-soluble material. Linkage analysis of the ethanol-insoluble fraction showed that it was devoid of Man*p*, but contained mostly 4-Glc*p* (31 mol%) and 4,6-Glc*p* (23 mol%), terminal Xyl*p* (14 mol%) and 2-Xyl*p* (17 mol%) and terminal Ara*f* (12 mol%)

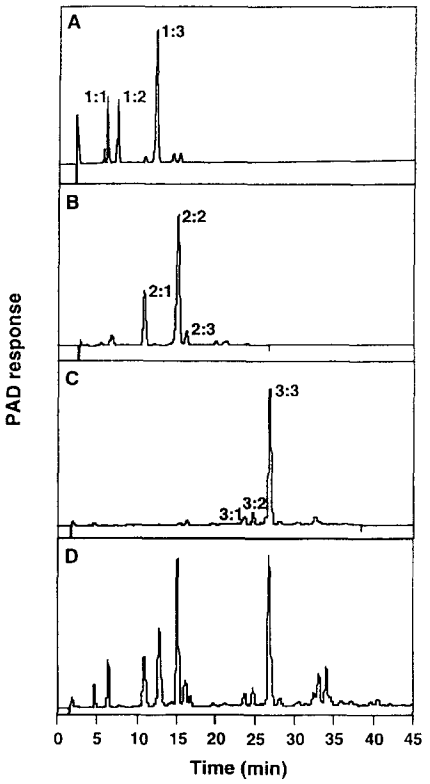

Fig. 2. Anion-exchange HPLC of native *Nicotiana plumbaginifolia* GGM digested with endo-(1 → 4)-β-mannanase. The oligosaccharides were separated on a CarboPac PA-1 column equilibrated in 150 mM NaOH and eluted with a 100-min linear gradient of NaOAc (0–250 mM) starting 5 min after sample injection. The eluted material was detected by pulsed amperometric detection. The elution profiles of oligosaccharides from peaks 1–3 (A–C, respectively) from gel-filtration chromatography (Fig. 1) was compared with total unfractionated native GGM oligosaccharides (D).

Table 2
Linkage composition of *Nicotiana plumbaginifolia* GGM oligosaccharides obtained by gel-filtration chromatography (Fig. 1) and by anion-exchange HPLC (Fig. 2)

Sugar	Deduced glycosidic linkage [a]	Linkage composition (mol%) [b,c]											
		Fraction											
		1	1:1	1:2	1:3	2	2:1	2:2	2:3	3	3:1	3:2	3:3
Ara*p*	Terminal	2	–	–	–	7	29	–	–	1	–	–	–
Xyl*p*	Terminal	2	–	–	–	2	–	–	23	2	–	14	–
	2-	–	–	–	–	–	–	–	–	3	–	–	–
Gal*p*	Terminal	5	–	6	–	26	4	34	10	22	24	19	27
	2-	2	–	–	–	–	–	–	–	13	13	7	14
Glc*p*	Terminal	40	32	–	56	37	30	33	28	16	9	18	14
	4-	3	6	tr	2	3	1	4	8	18	14	13	16
	4,6-	–	–	–	–	–	–	–	–	3	–	–	–
Man*p*	Terminal	15	62	55	–	–	3	–	tr	–	14	tr	–
	4-	28	–	35	41	3	–	2	1	3	4	2	3
	6-	–	–	3	–	–	–	–	2	–	–	tr	–
	4,6-	3	–	1	1	22	33	27	27	18	22	25	26

[a] Terminal Ara*p* is deduced from 1,5-di-*O*-acetyl-2,3,4-tri-*O*-methylpentitol, etc.
[b] Average of duplicate determinations.
[c] –, Not detected.

consistent with this fraction being XG [9]. Thus, all of the GGM was digested by the endo-(1 → 4)-β-mannanase since no GGM linkages were detected in the ethanol-insoluble fraction. In order to identify the oligosaccharides present in the ethanol-soluble fraction, the digest was separated by a combination of

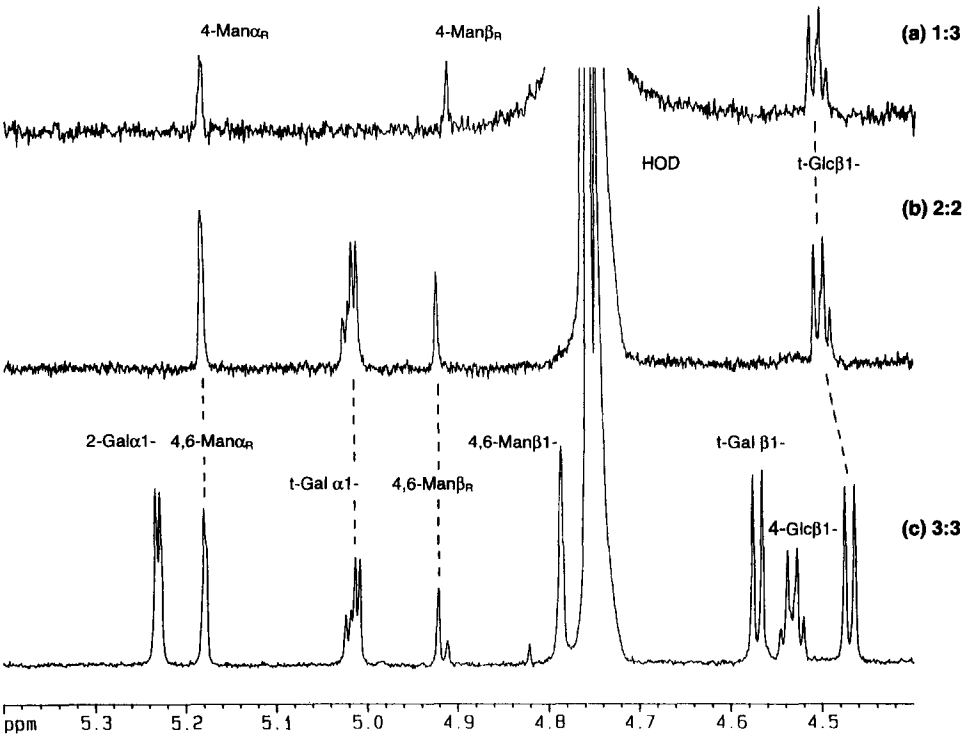

Fig. 3. ^{1}H NMR spectra of *Nicotiana plumbaginifolia* GGM oligosaccharide peaks 1:3 (a), 2:2 (b), and 3:3 (c). The spectra were recorded on a Bruker DMX750 spectrometer with a spectral width of 6000 Hz, 16K data points, 60° pulse, an acquisition time of 1.3 s, a relaxation delay of 3.3 s, and 32–512 scans.

gel-filtration chromatography and anion-exchange HPLC.

Chromatography of GGM oligosaccharides.—Gel-filtration chromatography on a Fractogel TSK HW-40 column of the ethanol-soluble products from *N. plumbaginifolia* native GGM digested with endo-(1 → 4)-β-mannanase for 24 h gave 4 peaks (Fig. 1). Peak 4 (16% of the ethanol-soluble products) contained partially digested GGM and some contaminating XG (data not shown); it was not analysed further. Peaks 1–3 were collected and were fractionated further by anion-exchange HPLC (Fig. 2A–C) and their elution profiles compared with those of total unfractionated native GGM oligosaccharides (Fig. 2D); the relative proportions of the fractions and individual oligosaccharides are given in relation to the total amount of GGM (89%) in the ethanol-soluble oligosaccharides. Material eluting after 30 min in total unfractionated native GGM oligosaccharides (Fig. 2D) represented partially digested GGM and contaminating XG oligosaccharides (data not shown). The structures of individual oligosaccharides isolated were determined by linkage analysis (Table 2), ESI–MS (Table 3) and ^{1}H NMR (Table 4, Fig. 3).

Structure of peak 1.—Peak 1 from the gel-filtration column (Fig. 1) constituted 17% (w/w) of the ethanol-soluble GGM from the endo-(1 → 4)-β-mannanase digest. Linkage analysis showed that this

Table 3
Quasimolecular ions from ESI–MS and relative proportions of oligosaccharides obtained from endo-(1 → 4)-β-mannanase digestion of native *Nicotiana plumbaginifolia* GGM

Peak (% EtOH-soluble digest) [a]	Peak from HPLC	Relative amount (%) [b]	Pseudomolecular ions $[M + Na]^+$		Composition glycosyl structure	Proposed
			Observed	Expected		
1 (17)	1:1	2	273.3	273	Hex	Glc*p* (40%) Man*p* (60%)
	1:2	3	477.5	477	Hex_2	**I** [c] (90%) **II** (10%)
	1:3	10	477.6	477	Hex_2	**III**
	Others	2				
2 (26)	2:1	6	638.2	637	Hex_2Pent	**IV** (75%)
			682.2		Hex_3	**V** (25%)
	2:2	17	681.9	681	Hex_3	**VI**
	2:3	1	638.3	637	Hex_2Pent	**VII** (86%)
			682.5	681	Hex_3	**VI** (14%)
	Others	2				
3 (52)	3:1	3	886.9	88	Hex_4	– [d]
			1090.3	1089	Hex_5	– [d]
			1294.6	1293	Hex_6	– [d]
			1499.0	1497	Hex_7	– [d]
	3:2	3	1454.7 [e]	1453	Hex_6Pent	**VIII**
	3:3	39	1294.6	1293	Hex_6	**IX** (30%)
			1499.0	1497	Hex_7	**X** (70%)
	Others	7				
Others		5				
Total		100				

[a] Relative proportion of each peak from gel-filtration chromatography (GFC) calculated from total carbohydrate determined by phenol–H_2SO_4 method [18]. These peaks accounted for 95% of the total ethanol-soluble material from the endo-(1 → 4)-β-mannanase digest of GGM, the remaining 5% comprising partially digested GGM.
[b] Relative proportion of each peak calculated from peak areas of individual components from anion-exchange HPLC (Fig. 2). These peaks accounted for 84% of the material in peaks 1–3 from gel-filtration chromatography, the remaining 11% comprising components present in minor amounts.
[c] Structures in text.
[d] –, Not determined.
[e] ESI–MS contains more than one quasimolecular ion, not included here for clarity (see text); Hex_6Pent was predominant (73%).

Table 4
^{1}H NMR chemical shifts (δ, ppm) of *Nicotiana plumbaginifolia* GGM oligosaccharides [a]

Sugar [b]		H-1	H-2	H-3	H-4	H-5	H-6	H-6′
Peak 1:3, deduced structure **III**								
→4)-Man*p*$_R$	(α)	5.18	3.98	–	–	–	–	–
	(β)	4.91	3.98	3.78	3.84	3.53	–	–
Glc*p*-β-(1→		4.50/4.51 [c]	3.32	3.51	3.42	3.51	3.73	3.93
Peak 2:1, deduced structures **IV** *(75%) and* **V** *(25%)*								
→4,6)-Man*p*$_R$	(α)	5.18	3.99	–	–	–	–	–
	(β)	4.92	3.99	–	–	–	–	–
Ara*p*-β-(1→		5.42	3.54	–	3.84 [d]	3.46/3.75 [d]	–	–
Gal*p*-α-(1→		4.99	3.84	3.90	4.02	3.90	–	–
Man*p*-β-(1→		4.74	–	–	–	–	–	–
Glc*p*-β-(1→		4.49/4.50 [c]	3.32	3.47	3.41	3.47	3.73	3.94
Peak 2:2, deduced structure **VI**								
→4,6)-Man*p*$_R$	(α)	5.18	3.99	3.96	3.91	4.09	3.33	–
	(β)	4.92	4.00	–	–	–	–	–
Gal*p*-α-(1→		5.01/5.02 [c]	3.83	3.91	4.01	3.89	3.70	–
Glc*p*-β-(1→		4.50/4.51 [c]	3.33	3.50	3.42	3.49	3.73	3.93
Peak 3:3, deduced structures **IX** *(30%) and* **X** *(70%)*								
→4)-Man*p*$_R$/→4,6)-Man*p*$_R$	(α)	5.18	3.99	–	3.91	4.09	3.33	–
→4)-Man*p*$_R$	(β)	4.91	–	–	–	–	–	–
→4,6)-Man*p*$_R$	(β)	4.92	4.00	–	–	–	–	–
Gal*p*-α-(1→		5.01/5.02 [c]	3.82	3.90	4.00	3.89	3.69	–
→4)Glc*p*-β-(1→		4.52/4.53 [c]	3.37	3.68	3.61	3.74	–	–
→4,6)-Man*p*-β-(1→		4.79	4.12	3.79	–	3.71	3.87	–
→2)-Gal*p*-α-(1→		5.23	3.94	4.05 [d]	4.17 [d]	4.16 [d]	3.83 [d]	–
Gal*p*-β-(1→		4.57	3.63 [e]	3.67 [e]	3.92	3.67 [e]	–	–
Glc*p*-β-(1→		4.47	3.32	3.49	3.40	3.50	3.73	3.92

[a] Measured relative to acetone at δ 2.225 ppm.
[b] Each sugar residue is in D-configuration.
[c] These_signals were split due to the influence of the two anomeric forms of reducing D-Man*p*.
[d] Shifts determined from TOCSY, but assignments may be interchanged.
[e] Indicates set of highly overlapped resonances.

peak contained mostly terminal Glc*p*, terminal Man*p* and 4-Man*p*, with smaller amounts of other residues (Table 2).

Anion-exchange HPLC of gel-filtration peak 1 yielded three major oligosaccharide peaks comprising 89% of the total, 1:1 (retention time [RT] 4.6 min, 13% w/w), 1:2 (RT 6.3 min, 18% w/w) and 1:3 (RT 12.8 min, 58% w/w) together with several minor components (< 3% w/w each) which were not collected for analysis (Fig. 2A). Peak 1:1 co-chromatographed on anion-exchange HPLC with Man and Glc, and ESI–MS of methylated peak 1:1 gave a quasimolecular ion at 273.3 amu, corresponding to Hex (Table 3). Linkage analysis showed that this peak contained terminal Man*p* and terminal Glc*p* in the approximate molar ratio of 2:1 (Table 2), indicating that this peak was composed mostly of mannose (60%) and glucose (40%). Peak 1:2 co-chromatographed on anion-exchange HPLC with mannobiose, and ESI–MS of methylated peak 1:2 yielded a quasimolecular ion at 477.5 amu, corresponding to Hex_2 (Table 3). Linkage analysis contained predominantly terminal Man*p* and 4-Man*p* (Table 2) in the molar ratio 1:0.64, slightly less than the 1:1 expected for mannobiose (structure **I**; 90% peak 2:1), together with smaller amounts of terminal Gal*p* and 6-Man*p* which indicated the presence of a minor amount (10%) of structure **II**. The reducing-end Manp residues are assumes to be in the β-configuration due to the specificity of the endo-(1→4)-β-mannanase.

D-Man*p*-β-(1→4)-D-Man*p*-β-(1→
I

D-Gal*p*-α-(1→6)-D-Man*p*-β-(1→
II

ESI–MS of methylated peak 1:3 also yielded a quasimolecular ion at 477.6 amu, corresponding to Hex_2 (Table 3), and linkage analysis contained terminal Glc*p* and 4-Man*p* in the molar ratio 1:0.75,

slightly less than the expected 1:1 ratio corresponding to Glc*p*-(1 → 4)-Man*p* (Table 2). The ^{1}H NMR spectrum of 1:3 was consistent with structure **III**; the anomeric region of the spectrum is shown in Fig. 3a. Chemical shifts for the non-anomeric signals in 1:3 were assigned from a 2D TOCSY spectrum, and both the anomeric and non-anomeric chemical shifts are reported in Table 4. The chemical shifts (δ) for H-1 of → 4)-D-Man*p*$_R$ (α, 5.18 ppm; β, 4.91 ppm) were assigned by comparison with spectral data for monosaccharides [21] and with data for digalactosylmannopentaose (D-Man*p*-β-(1 → 4)-[D-Gal*p*-α-(1 → 6)]-D-Man*p*-β-(1 → 4)-[D-Gal*p*-α-(1 → 6)]-D-Man*p*-β-(1 → 4)-D-Man*p*-β-(1 → 4)-D-Man*p*) [22]. The chemical shifts of the H-1 doublet for terminal β-D-Glc*p* (4.51 ppm, *J* 7.8 Hz) were assigned by comparison with spectral data for XG oligosaccharides from *N. tabacum* [23]. The signal for terminal β-D-Glc*p* contained a second overlapping doublet (δ 4.50) having an intensity approximately one-third of the major peak. This is attributed to the sensitivity of terminal β-D-Glc*p* residue to the α/β anomers of the adjacent Man*p* which occur in a ratio of α:β of ~ 3:1. Such an anomerisation effect has been reported previously in NMR spectra for residues adjacent to the reducing-end of oligosaccharides [22]. From the susceptibility of GGM to endo-(1 → 4)-β-mannanase the → 4)-D-Man*p*$_R$ residue is in the β-configuration in the polysaccharide and is assigned in this way in structure **III**. The same logic applies to assignments of the D-Man*p*$_R$ residues in all subsequent structures.

D-Glc*p*-β-(1→4)-D-Man*p*-β-(1→
III

Structure of peak 2.—Peak 2 from the gel-filtration column (Fig. 1) comprised 26% (w/w) of the ethanol-soluble GGM from the endo-(1 → 4)-β-mannanase digest. Linkage analysis showed it contained mostly terminal Gal*p*, terminal Glc*p* and 4,6-Man*p*, with smaller amounts of terminal Ara*p*, terminal Xyl*p*, 4-Glc*p* and 4-Man*p* (Table 2).

Anion-exchange HPLC of gel-filtration peak 2 yielded three major oligosaccharide peaks comprising 93% of the total, 2:1 (RT 10.9 min, 22% w/w), 2:2 (RT 15.2 min, 65% w/w), and 2:3 (RT 16.2 min, 6% w/w) together with several minor components (< 3% w/w each) which were not collected for analysis (Fig. 2B). ESI–MS of methylated peak 2:1 yielded a major quasimolecular ion at 638.2 amu (75%; Table 3) corresponding to Hex_2Pent. Linkage analysis of peak 2:1 contained predominantly terminal Ara*p*, terminal Glc*p* and 4,6-Man*p* in the molar ratio of 1.0:1.0:1.1 (Table 2), which was consistent with this peak comprising predominantly Glc*p*-(1 → 4)-[Ara*p*-(1 → 6)]-Man*p*. The presence in the ESI–MS of a second quasimolecular ion at 682.2 amu (25%) corresponding to Hex_3 and of small amounts of terminal Gal*p*, terminal Man*p* and the excess 4,6-Man*p* in the linkage analysis of peak 2:1 (Table 2) indicated that the Hex_3 component of peak 2:1 was Man*p*-(1 → 4)-[Gal*p*-(1 → 6)]-Man*p*.

The NMR spectrum of peak 2:1 is consistent with structure **IV**, in that the signals for Ara*p*, Glc*p* and Man*p* are detected (Table 4). The anomeric region shows the presence of → 4,6)-D-Man*p*$_R$ (α, 5.18 ppm; β, 4.92 ppm) and terminal β-D-Glc*p* (4.49/4.50 ppm). An anomeric signal at 5.42 ppm was attributed to a terminal D-Ara*p* in the β-configuration, based on the chemical shifts of terminal Ara*p* (5.35–5.36 ppm) of lipophosphoglycan oligosaccharides from *Leishmania major* which was initially deduced to be in the α-configuration [24], but was later reassigned as the β-configuration [25]. In addition, Mizutani et al. [26] noted that the chemical shifts of arabinopyranosides are characteristic of the anomeric configuration, with H-1 for β-arabinopyranosides occurring in the range 5.00–5.50 ppm and those for α-arabinopyranosides in the range 4.58–4.72 ppm. The observed coupling of 3.4 Hz is also consistent with the β-configuration. Mizutani et al. [26] noted that $J_{1,2}$ is consistently ~ 3 Hz for a β series and 7 Hz for an α series of L-arabinopyranosides. Integration of the anomeric signals indicated that the relative intensities of signals for terminal β-D-Ara*p* and terminal β-D-Glc*p* were similar to each other, but were smaller than that for → 4,6)-D-Man*p*$_R$. A doublet (*J* ~ 3.4 Hz) at 4.99 ppm was consistent with the presence of terminal α-D-Gal*p*, and a peak at 4.74 ppm (resolved from the residual water resonance by running the spectrum at 37 °C) was tentatively identified as terminal β-D-Man*p* by comparison with the chemical shifts for digalactosylmannopentaose [22]. These signals, together with the intensity of the → 4,6)-D-Man*p*$_R$ (from both structures **IV** and **V**) signals higher than for terminal β-D-Ara*p* and terminal β-D-Glc*p*, were consistent with peak 2:1 containing structure **V**. The ratio of structures **IV** and **V**, determined from NMR signals for terminal β-D-Glc*p* (from structure **IV**) and terminal β-D-Man*p* (from structure **V**) was ~ 1.5:1, whereas the ratio of **IV**:**V** obtained from ESI–MS was 3:1. We are uncertain of why this anomaly

exists, but in order to calculate their relative proportions in GGM we have taken the ratio to be 2:1, the approximate average of the two techniques.

D-Glc*p*-β-(1→4)-D-Man*p*-β-(1→
6
↑
1
D-Ara*p*-β

IV

D-Man*p*-β-(1→4)-D-Man*p*-β-(1→
6
↑
1
D-Gal*p*-α

V

ESI–MS of methylated peak 2:2 yielded a quasimolecular ion at 681.9 amu corresponding to Hex_3 (Table 3). The glycosyl composition of peak 2:2 contained mostly terminal Gal*p*, terminal Glc*p* and 4,6-Man*p* in the approximate molar ratio of 1:1:1 (Table 2), and thus this peak was identified as Glc*p*-(1 → 4)-[Gal*p*-(1 → 6)]-Man*p*. The ^{1}H NMR spectrum of peak 2:2 was consistent with structure **VI**; the anomeric region shown in Fig. 3b confirms the presence of → 4,6)-D-Manp_R (α, 5.18 ppm; β, 4.92 ppm) together with terminal β-D-Glc*p* (4.50/4.51 ppm) and terminal α-D-Gal*p* (5.01/5.02 ppm) (Table 4). The latter two residues are each associated with overlapping sets of doublets as a result of the anomerisation effect of the adjacent reducing 4,6-Man*p* residue [22]. In the case of the terminal β-D-Glc*p* anomeric signal, the minor component (corresponding to the β-configuration of the adjacent Man*p* residue) is upfield of the main signal whereas in the case of the terminal α-D-Gal*p* it is downfield. It is also interesting to note that the H-1 signal for → 4,6)-D-Manp_R in the β-configuration in structure **VI** occurs slightly downfield (by 0.01 ppm) of its position in structure **III**, which can be attributed to substitution of the Man*p* residue at O-6 by Gal*p*. The effect is significantly smaller for the H-1 signal of Man*p* in the α-configuration, so the shifts of H-1 for this residue are essentially superimposed in structures **III** and **VI**. The complete chemical shift assignments for H-1 to H-6 of the Man, Glc and Gal residues of 2:2 determined from the 2D TOCSY spectra are reported in Table 4.

D-Glc*p*-β-(1→4)-D-Man*p*-β-(1→
6
↑
1
D-Gal*p*-α

VI

Linkage analysis of peak 2:3 contained an approximate 1:1 molar ratio of terminal Glc*p* and 4,6-Man*p*, together with terminal Xyl*p* and terminal Gal*p* (Table 2). ESI–MS of methylated peak 2:3 yielded a quasimolecular ion at 638.3 amu (86%) corresponding to Hex_2Pent, and a second, less intense quasimolecular ion at 682.5 amu (14%) corresponding to Hex_3 (Table 3). The presence of terminal Glc*p*, 4,6-Man*p*, and terminal Xyl*p* was consistent with the major component of peak 2:3 being Glc*p*-(1 → 4)-[Xyl*p*-(1 → 6)]-Man*p* which was deduced to be structure **VII** (~ 69%); the presence of terminal Gal*p* and a quasimolecular ion at *m/z* 682.5 deduced to be carried over from peak 2:2 (see Fig. 2B). We presume that the terminal Xyl*p* residues are α-linked based on homology to the α-Gal*p* residues in GGMs, isolated as part of this study, in previous studies [5–7], and to the α-Xyl*p* residues in XGs [9,16,23].

D-Glc*p*-β-(1→4)-D-Man*p*-β-(1→
6
↑
1
D-Xyl*p*

VII

Structure of peak 3.—Peak 3 from the gel-filtration column (Fig. 1) comprised 52% (w/w) of the ethanol-soluble GGM from the endo-(1 → 4)-β-mannanase digest. Linkage analysis showed it contained mostly terminal Glc*p* and 4-Glc*p*, 4,6-Man*p* and terminal Gal*p* and 2-Gal*p*, with smaller amounts of other linkages (Table 2).

Anion-exchange HPLC of gel-filtration peak 3 yielded three individual oligosaccharides comprising 88% of the total, 3:1 (RT 23.7 min, 6% w/w), 3:2 (RT 24.7 min, 6% w/w), and 3:3 (RT 26.8 min 77% w/w) together with several minor components (< 2% w/w each) which were not collected for analysis (Fig. 2C). Linkage analysis of peak 3:1 contained terminal Gal*p* and 2-Gal*p*, terminal Glc*p* and 4-Glc*p*, terminal Man*p*, 4-Man*p* and 4,6-Man*p* (Table 2). ESI–MS of methylated peak 3:1 was complex, yielding quasimolecular ions at 886.9, 1090.3, 1294.6, and 1499.0 amu, corresponding to oligosaccharides Hex_{4-7} (Table 3). These data showed that peak 3:1 contained a mixture of oligosaccharides, but as there was insufficient material to isolate each component the individual oligosaccharides were not identified.

ESI–MS of methylated peak 3:2 yielded a major quasimolecular ion at 1454.7 amu (~ 73% of this peak; Table 3) corresponding to Hex_6Pent, and minor

quasimolecular ions at 886.8, 1045.9, 1089.8, and 1250.9 amu corresponding to Hex_4, Hex_4Pent, Hex_5, and Hex_5Pent, respectively. The linkage analysis of peak 3:2 contained terminal Xyl*p*, terminal Gal*p* and 2-Gal*p*, terminal Glc*p* and 4-Glc*p*, and 4,6-Man*p* (Table 2) in proportions 1.1:1.4:0.6:1.4:1.0:2.0, suggesting that the major (73%) component of peak 3:2 was Glc*p*-(1 → 4)-[Gal*p*-(1 → 2)-Gal*p*-(1 → 6)]-Man*p*-(1 → 4)-Glc*p*-(1 → 4)-[Xyl*p*-(1 → 6)]-Man*p* which was deduced to be structure **VIII** assuming an alternating Glc–Man backbone (see structures **IX** and **X**) and from the treatment of GGM with α- and β-galactosidases. However, the small amount of this peak did not allow further analysis, and several unidentified components were also present.

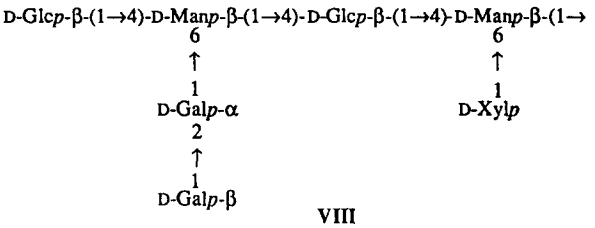

VIII

ESI–MS of methylated peak 3:3 yielded quasimolecular ions at 1294.6 (30%) and 1499.0 amu (70%; Table 3) corresponding to the presence of Hex_6 and Hex_7, respectively. Linkage analysis of peak 3:3 contained terminal Gal*p* and 2-Gal*p*, terminal Glc*p* and 4-Glc*p*, and 4,6-Man*p* in the molar ratio of 2.0:1.0:1.0:1.2:1.9, together with a small amount of 4-Man*p* (molar ratio 0.2; Table 2). In order to identify unambiguously the primary structure of peak 3:3 components, 1D and 2D ^1H NMR spectra were acquired. The anomeric region of the 1D spectrum is shown in Fig. 3c, and the ^1H chemical shifts for the glycosyl ring systems present in peak 3:3 are given in Table 4. The chemical shifts for H-1 of the → 4)-D-Manp_R and → 4,6)-D-Manp_R were assigned by comparison with data for structures **III** and **VI**, purified in this study, and with data for digalactosylmannopentaose [22]. As noted previously, the chemical shift for H-1 for → 4)-D-Manp_R in the β-configuration from structure **III** (4.91 ppm) was slightly upfield of H-1 of → 4,6)-D-Manp_R in the β-configuration from structure **VI** (4.92 ppm), while the chemical shifts for both → 4)-D-Manp_R and → 4,6)-D-Manp_R in the α-configuration overlapped (5.18 ppm). In the 1D spectrum of peak 3:3 (Fig. 3c), the presence of anomeric protons at δ 4.91 ppm [→ 4)-D-Manp_R, **IX**] and 4.92 ppm [→ 4,6)-D-Manp_R, **X**] indicated that two oligosaccharides, with a branched (76%, from relative intensities of peaks) and unbranched (24%) reducing Man*p* residue, respectively, were present.

We had observed previously (e.g. structures **III** and **VI**) that the H-1 signals of glycosyl residues adjacent to the reducing-end Man*p* residues [→ 4)-D-Manp_R and → 4,6)-D-Manp_R] were split due to the anomerisation effect of the reducing-end residue, similar to that observed for digalactosylmannopentaose [22]. Thus, in conjunction with established data on the chemical shifts of similar residues in digalactosylmannopentaose [22] and XG [23] we were able to assign the split H-1 signals in peak 3:3 to a terminal α-D-Gal*p* (5.01/5.02 ppm) on the → 4,6)-D-Manp_R residue in structure **X** and to a → 4)-β-D-Glc*p* (4.52/4.53 ppm) residue adjacent to the reducing-end Man*p* in structures **IX** and **X**. Similar comparisons also enabled the chemical shifts for terminal β-D-Glc*p* (**IX** and **X**, 4.47 ppm), terminal β-D-Gal*p* (**IX** and **X**, 4.57 ppm) and → 4,6)-β-D-Man*p* (**IX** and **X**, 4.79 ppm) to be assigned from the 1D spectrum, and the remaining signal at δ 5.23 ppm was deduced to be due to the anomeric proton of → 2)-α-D-Gal*p* (**IX** and **X**). These assignments were confirmed from an analysis of 2D TOCSY and DQF-COSY spectra. The shifts for H-2 to H-6 reported in Table 4 are consistent with those seen in analogous oligosaccharides [16,22,23].

Identification of the → 4)-D-Manp_R and → 4,6)-D-Manp_R with the adjacent → 4)-D-Glc*p*, and the → 4,6)-D-Man*p* and terminal β-D-Glc*p*, showed that the oligosaccharides in peak 3:3 consisted of an alternating Glc*p*–Man*p* backbone. The relative intensities of signals for → 2)-α-D-Gal*p* and terminal β-D-Gal*p* were similar to that of → 4,6)-D-Man*p*, which indicated that the disaccharide Gal*p*-β-(1 → 2)-Gal*p*-α-(1 → was attached to → 4,6)-D-Man*p*. Thus, from the ^1H NMR and the linkage analysis data the Hex_6 structure in peak 3:3 was identified as structure **IX** (~ 30% of this peak), and the Hex_7 structure was identified as structure **X** (~ 70%).

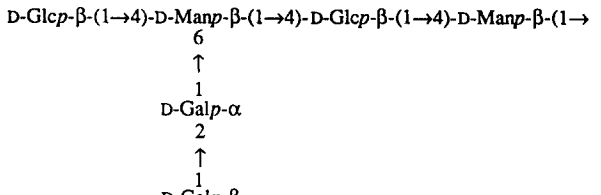

IX

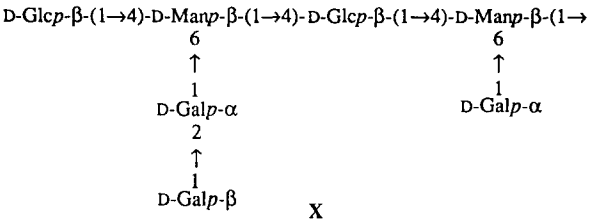

X

4. Conclusions

In this study the structure of the major subunits of GGM isolated from the extracellular medium of suspension cultures of *N. plumbaginifolia* have been determined. The GGM has a similar primary structure to that from *N. tabacum* leaves and suspension cultures [5,6]. The backbone of predominantly alternating →4)-D-Man*p*-β-(1→ and →4)-D-Glc*p*-β-(1→ residues (see Scheme 1) is branched at O-6 of 65% of the Man*p* residues to either single Gal*p*-α-(1→ residues (~38 mol% of branches), or the disaccharide Gal*p*-β-(1→2)-Gal*p*-α-(1→ (~42 mol%) or, less commonly, to Ara*p*-β-(1→ (~13 mol%) or Xyl*p*-α-(1→ (~7 mol%). Low proportions of Ara and Xyl have been detected previously in GGM preparations from *N. tabacum* [5,6], although these residues were absent from endo-(1→4)-β-glucanase digests, and therefore assumed to be from contaminating molecules (e.g. arabinoxyloglucan). Thus, this is the first study in which terminal Ara*p* and terminal Xyl*p* have been shown to be attached to O-6 of the 4-Man*p* residues in the backbone of GGM. The majority (70%) of the GGM is composed of oligosaccharide structures **III** (10%), **IV** (4%), **VI** (17%), **IX** (12%), and **X** (27%), with smaller amounts of structures **I** (3%), **V** (2%), **VII** (1%), and **VIII** (2%). Methylation of native GGM under neutral conditions showed that *O*-acetyl groups are present at the C-6 position of a small proportion of the terminal Gal*p* and 4-Man*p* residues, equivalent to a total degree of *O*-acetylation of ~0.8%. Since it was only possible to separate the individual oligosaccharide isomers by high-pH anion-exchange HPLC for this detailed structural characterisation we were unable to comment on the distribution of these *O*-acetyl groups on the GGM in the model proposed below.

From the structural requirements of galactomannans and GGMs for binding to endo-(1→4)-β-mannanase, and the structure of the GGM oligosaccharides obtained in this present study, one of a number of possible models for *N. plumbaginifolia* GGM and the hydrolysis by *A. niger* endo-(1→4)-β-mannanase is proposed (see Scheme 1). The enzymic hydrolysis of (galacto)mannans by endo-(1→4)-β-mannanase has been studied extensively (refs [2,27] and references therein). In a detailed study, the endo-(1→4)-β-mannanase from *A. niger* was shown to readily hydrolyse Man_5 and Man_6, whereas Man_4 was hydrolysed slowly and Man_3 was resistant to hydrolysis [28]. The enzyme was shown to bind to five Man*p* residues in the active site ($_{NR}\alpha$–β–χ–δ–ϵ_R), and cleave the β-(1→4)-glycosidic bond between the second (δ) and third (χ) Man*p* residues from the reducing-end of the pentosyl unit. The *A. niger* endo-(1→4)-β-mannanase may also bind to four Man*p* residues, and differences in the rate of hydrolysis of two galactosylmannotetraoses (D-Man*p*-β-(1→4)-[D-Gal*p*-α-(1→6)]-D-Man*p*-β-(1→4)-D-Man*p*-β-(1→4)-D-Man*p* and [D-Gal*p*-α-(1→6)]-D-Man*p*-β-(1→4)-D-Man*p*-β-(1→4)-D-Man*p*-β-(1→4)-D-Man*p*) indicate that binding to the ϵ residue is more important than binding to the α residue [28]. However, the hydrolysis of Man_5 occurs at a faster rate than Man_4, indicating that presence of both the α and ϵ residues is preferred. The two-fold screw axis of the backbone of (galacto)mannans means that hydroxymethyl groups ($-CH_2OH$) on neighbouring Man*p* residues are on opposite sides of the chain. Substitution of the Man*p* backbone by single Gal*p* residues on alternate Man*p* residues has no effect on enzyme–substrate interaction, although substitution of the second Man*p* (δ) residue from the reducing-end of the enzyme-binding site blocks binding, but substitution of the third Man*p* (χ) residue does not. Thus, digestion of galactomannan with endo-(1→4)-β-mannanase often produces oligosaccharides where the reducing-end Man*p* residues are substituted [27,28]. In this present study GGM oligosaccharides were obtained where the reducing-end Man*p* residues were substituted at O-6 with either Gal*p*-α-(1→, or Ara*p*-β-(1→, or Xyl*p*-α-(1→, but not with Gal*p*-β-(1→2)-Gal*p*-α-(1→, suggesting that substitution of the third Man*p* (χ) residue from the reducing-end of the enzyme-binding site with this disaccharide blocks the binding and action of the enzyme.

Enzymic hydrolysis of glucomannan [2,27,28] shows that only Man*p* is obtained as the reducing-end residue, indicating that the configuration of this residue (χ) is important for binding of the enzyme. In this present study, the majority of the GGM oligosaccharides obtained following digestion with endo-(1→4)-β-mannanase contained either two or four backbone glycosyl residues, with only Man*p* as the

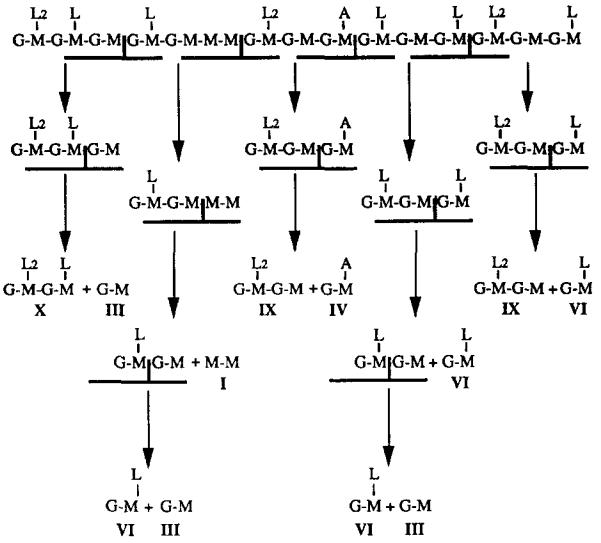

Scheme 1. Nomenclature: G, →4)-β-D-Glc*p*(1→; M, →4)-β-D-Man*p*(1→; L, D-Gal*p*-α-(1→; A, Ara*p*-β-(1→; L_2, D-Gal*p*-β-(1→2)-D-Gal*p*-α-(1→; ⊥, enzyme-binding site and position of cleavage.

reducing-end residue; the predominant non-reducing terminal residue was Glc*p*. The requirement for at least four glycosyl residues for binding of the backbone to the enzyme, together with the ~2.7:1 molar ratio of oligosaccharides with two (structures **I–VII**) and four (structures **VIII–X**) glycosyl residues, suggests that digestion of GGM could occur predominantly via intermediates of six backbone glycosyl residues with predominantly alternating →4)-D-Man*p*-β-(1→ and →4)-D-Glc*p*-β-(1→ residues (see Scheme 1). On the backbone of predominantly alternating Man*p* and Glc*p* residues the disaccharide Gal*p*-β-(1→2)-Gal*p*-α-(1→ substituents would be regularly spaced every twelve residues. The precise distribution of the single glycosyl substituents is unclear, but would probably be regularly spaced along the backbone.

If cleavage of GGM occurs predominantly through the *A. niger* endo-(1→4)-β-mannanase binding to four Man*p* residues instead of five, then the precise mechanism of hydrolysis and sequence may vary from that shown in Scheme 1.

The presence of GGM in the ECPs of suspension-cultured *N. plumbaginifolia* is consistent with the presence of this molecule in the primary walls of these cells, similar to that found in ECPs and walls of suspension-cultured *N. tabacum* [5,6] and *Rubus fruticosus* [7] cells. However, the incorporation of GGM into the three-dimensional matrix of these walls is not understood. The similarity of the backbone of GGM to XG suggests that GGM may be able to hydrogen bond to cellulose. The degree of glycosyl substitution of the backbone of *N. plumbaginifolia* GGM is ~35%, which is slightly lower than the degree of glycosyl substitution of XG (~40%) secreted into the medium of suspension culture of this species [8]. However, the backbone of GGM probably has a predominantly alternating glycosyl substitution pattern, which results in a molecule with one unsubstituted face (see Scheme 1), whereas XG has a regular pattern of two consecutive backbone residues xylosylated (on opposite sides of the chain) and two or three backbone residues non-xylosylated [9]. Further, many of the non-xylosylated 4-Glc*p* residues of *N. plumbaginifolia* XG are substituted with *O*-acetyl groups, whereas the GGM has only a low degree of *O*-acetylation. Study of the interaction between GGM and cellulose in vitro, similar to that for XG and cellulose [29,30] may give insights into the role of GGM in primary cell walls.

Acknowledgements

We thank Dr. David McManus for the production and supply of ECPs from *N. plumbaginifolia*, Dr. Graeme Currie for assistance with ESI–MS and Dr. Steve Read for critical assessment of the manuscript. This research was supported by funds from a Cooperative Research Centre Program of the Commonwealth Government of Australia to the CRC for Industrial Plant Biopolymers, and the ESI–MS was purchased with grants from the University of Melbourne, the Australian Research Council, the Clive and Vera Ramaciotti Foundation and the Ian Potter Foundation. D.J.C. is an Australian Research Council Professorial Fellow.

References

[1] A. Bacic, P.J. Harris, and B.A. Stone, in J. Priess (Ed.), *The Biochemistry of Plants, A Comprehensive Treatise*, Vol. 14, Academic Press, New York, 1988, pp. 297–371.
[2] N.K. Matheson, in P.M. Dey and J.B. Harborne (Eds), *Methods in Plant Biochemistry*, Vol 2, Academic Press, New York, 1990, pp. 371–413.
[3] M. Kubackova, S. Karakonyi, and L. Bilisics, *Carbohydr. Polym.*, 19 (1992) 125–129.
[4] G.O. Aspinall, in W. Tanner and F.A. Loewus (Eds), *Encyclopedia of Plant Physiology*, Vol 13B, Springer, Berlin, 1981, pp. 3–8.
[5] Y. Akiyama, S. Eda, M. Mori, and K. Kato, *Phytochemistry*, 22 (1983) 1177–1180.

[6] S. Eda, Y. Akiyama, K. Kato, A. Ishizu, and J. Nakano, *Carbohydr. Res.*, 137 (1985) 173–181.
[7] N. Cartier, G. Chambat, and J.-P. Joseleau, *Phytochemistry*, 27 (1988) 1361–1364.
[8] I.M. Sims and A. Bacic, *Phytochemistry*, 38 (1995) 1397–1405.
[9] I.M. Sims, S.L.A. Munro, G. Currie, D. Craik, and A. Bacic, *Carbohydr. Res.*, 293 (1996) 147–172.
[10] H. Schlüpmann, A. Bacic, and S.M. Read, *Planta*, 191 (1993) 70–81.
[11] M. Dubois, K.A. Gilles, J.K. Hamilton, P.A. Rebers, and F. Smith, *Anal. Chem.*, 28 (1956) 350–356.
[12] S.M. Read, G. Currie, and A. Bacic, *Carbohydr. Res.*, 281 (1995) 187–201.
[13] I. Ciucanu and F. Kerek, *Carbohydr. Res.*, 131 (1984) 209–217.
[14] P. Prehm, *Carbohydr. Res.*, 78 (1980) 372–374.
[15] E. Lau and A. Bacic, *J. Chromatogr.*, 637 (1993) 100–103.
[16] W.S. York, L.K. Harvey, R. Guillen, P. Albersheim, and A.G. Darvill, *Carbohydr. Res.*, 248 (1993) 285–301.
[17] D. Marion and K. Wüthrich, *Biochem. Biophys. Res. Comm.*, 113 (1983) 967–974.
[18] M. Rance, O.W. Sørenson, G. Bodenhausen, G. Wagner, R.R. Ernst, and K. Wüthrich, *Biochem. Biophys. Res. Comm.*, 117 (1983) 479–485.
[19] L. Braunschweiler and R.R. Ernst, *Mol. Phys.*, 53 (1983) 521–528.
[20] D.G. Davis and A. Bax, *J. Am. Chem. Soc.*, 107 (1985) 2820–2821.
[21] P.K. Agrawal, *Phytochemistry*, 31 (1992) 3307–3330.
[22] A.L. Davis, R.A. Hoffman, A.L. Russell, and M. Debet, *Carbohydr. Res.*, 271 (1995) 43–54.
[23] W.S. York, V.S. Kumar Kolli, R. Orlando, P. Albersheim, and A.G. Darvill, *Carbohydr. Res.*, 285 (1996) 99–128.
[24] M.J. McConville, J.E. Thomas-Oates, M.A.J. Ferguson, and S.W. Homans, *J. Biol. Chem.*, 32 (1990) 19611–19623.
[25] M.J. McConville and M.A.J. Ferguson, *Biochem. J.*, 294 (1993) 305–324.
[26] K. Mizutani, R. Kasai, and O. Tanaka, *Carbohydr. Res.*, 87 (1980) 19–26.
[27] N.K. Matheson and B.V. McCleary, in G.O. Aspinall (Ed.), *The Polysaccharides*, Vol 3, Academic Press, New York, 1985, pp. 1–105.
[28] B.V. McCleary and N.K. Matheson, *Carbohydr. Res.*, 119 (1983) 191–219.
[29] T. Hayashi, K. Ogawa, and Y. Mitsuichi, *Plant Cell Physiol.*, 35 (1994) 1199–1205.
[30] S.E.C. Whitney, J.E. Brigham, A.H. Darke, J.S.G. Reid, and M.J. Gidley, *Plant J.*, 8 (1995) 491–504.